Low-Energy Electronic Properties of Clean $CaRuO_3$: Elusive Landau Quasiparticles

M. Schneider,[1] D. Geiger,[2,*] S. Esser,[1,†] U. S. Pracht,[2] C. Stingl,[1] Y. Tokiwa,[1] V. Moshnyaga,[1] I. Sheikin,[3] J. Mravlje,[4] M. Scheffler,[2] and P. Gegenwart[1,†]

[1]*I. Physikalisches Institut, Georg-August-Universität Göttingen, D-37077 Göttingen, Germany*

[2]*1. Physikalisches Institut, Universität Stuttgart, D-70550 Stuttgart, Germany*

[3]*Laboratoire Nationale des Champs Magnétiques Intenses, 25 Rue des Martyrs, 38042 Grenoble, France*

[4]*Josef Stefan Institute, SI-1000 Ljubljana, Slovenia*

(Received 13 December 2013; published 23 May 2014)

We have prepared high-quality epitaxial thin films of $CaRuO_3$ with residual resistivity ratios up to 55. Shubnikov–de Haas oscillations in the magnetoresistance and a T^2 temperature dependence in the electrical resistivity only below 1.5 K, the coefficient of which is substantially suppressed in large magnetic fields, establish $CaRuO_3$ as a Fermi liquid (FL) with an anomalously low coherence scale. At $T > 1.5$ K non-Fermi-liquid (NFL) behavior is found in the electrical resistivity. The high sample quality allows access to the intrinsic electronic properties via THz spectroscopy. For frequencies below 0.6 THz, the conductivity is Drude-like and can be modeled by FL concepts; for higher frequencies, non-Drude behavior is found, which is inconsistent with FL predictions. This establishes $CaRuO_3$ as a prime example of optical NFL behavior in the THz range.

DOI: 10.1103/PhysRevLett.112.206403 PACS numbers: 71.10.Hf, 71.27.+a, 74.70.Pq

Landau Fermi liquid (FL) theory assumes a one-to-one correspondence of electronic excitations in metals [so-called quasiparticles (QPs)] to those of the noninteracting Fermi gas. Remarkably, FL behavior persists in materials where the electronic interactions are strong; however, this often occurs only below a low FL temperature T_{FL}. FL theory is the established framework that describes metallic behavior in a broad class of materials, ranging from elemental metals to correlated oxides and heavy-fermion systems. Therefore, metals that behave inconsistently with FL predictions attract a lot of attention. A quasilinear, instead of a FL-predicted quadratic, temperature dependence of the electrical resistivity is found in heavy-fermion metals near a magnetic quantum critical point (QCP) and in high-T_c superconductors at optimal doping [1–3]. It is controversial whether such non-Fermi-liquid (NFL) behavior arises due to the interaction of the QPs with low-energy magnetic excitations near QCPs, or whether the QP picture needs to be abandoned completely [4].

NFL behavior has also been discussed in certain ruthenates. Unlike the heavy-fermion compounds and cuprates, these are characterized by broad electronic bands (with bandwidth $W \sim 3$ eV) and small interaction strength $U \lesssim W$. The optical conductivity of $SrRuO_3$ and $CaRuO_3$ in the infrared exhibits an unusual frequency dependence $\sigma_1 \propto \omega^{-0.5}$ [5,6], while time-domain THz measurements found signs of an unconventional metallic response at lower frequency [7]. However, disorder strongly influences the properties of ruthenates [8] and FL behavior was observed in sufficiently clean samples of $SrRuO_3$. $CaRuO_3$ was argued to be positioned right at a magnetic QCP, as signified by a logarithmic term in the specific heat coefficient and an electrical resistivity $(\rho(T) - \rho_0) \propto T^{3/2}$ (ρ_0 is the residual resistivity) below 30 K [8,9]. Since paramagnetic $CaRuO_3$ crystallizes in the same orthorhombically distorted perovskite structure as the isoelectronic itinerant ferromagnet $SrRuO_3$ [10,11], proximity to a ferromagnetic instability indeed seems plausible. The substitution of Sr by Ca in $Sr_{1-x}Ca_xRuO_3$ results in a suppression of the ordering beyond $x \approx 0.7$ [10,12–14]. This is associated with a drastic softening of magnetic exchange [15,16]. First-principles band structure calculations indicate that $CaRuO_3$ is located close to a ferromagnetic instability and paramagnonlike spin excitations are very soft [15]. Ferromagnetic dynamical scaling has been found in NMR experiments, although the bulk susceptibility reveals a strongly negative Curie-Weiss temperature in $CaRuO_3$ [13].

Complementary insights into ruthenates have come from the dynamical mean-field theory (for a review, see Ref. [17]), which pointed out how the Hund's-rule coupling suppresses the coherence scale and induces strong electronic correlations, even in cases where $U \lesssim W$. Interestingly, even in such a local picture, NFL effects are found, with an ongoing debate about how much they can persist into the zero-temperature limit [17–19]. The material that might realize such a local NFL is $CaRuO_3$. In $CaRuO_3$, settling the question about intrinsic low-temperature properties is complicated by the involved crystal growth [10,20] that leads to insufficiently pure samples, contrary to the case of Sr_2RuO_4 [21] or $Sr_3Ru_2O_7$ [22].

Previously, thin films of $CaRuO_3$ have been synthesized by, e.g., sputtering and pulsed-laser deposition techniques [12,23–25]. However, the obtained residual resistivity ratio (RRR) values are only of order 5–10. Below, we

report the synthesis of high-purity $CaRuO_3$ thin films, the first observation of quantum oscillations, and a study of the mass enhancement in this material. Our results demonstrate a fragile FL ground state and robust NFL behavior in its vicinity. The coherence scale T_{FL} increases rapidly under an applied magnetic field, signaling a strong influence of spin fluctuations on the electronic properties. Low-temperature THz conductivity data follow Drude and FL predictions only below 0.6 THz, and reveal an abrupt increase of the optical scattering rate at higher frequencies.

Details of the $CaRuO_3$ thin film synthesis by the metal-organic aerosol deposition technique, as well as their characterization, are provided in the Supplemental Material [26]. An important improvement of the sample quality has been obtained by using (110) oriented $NdGaO_3$ (NGO) substrates with 3° miscut angle, yielding RRR values up to 55, which is comparable to the best $SrRuO_3$ thin films [27]. Figure 1(a) displays the temperature dependence of the electrical resistivity of a $CaRuO_3$ thin film. The surface morphology shown by a scanning tunneling microscopy (STM) image [Fig. 1(b)] clearly indicates a step-bunching growth mode with steps of about 10 nm height and 220 nm lateral extension, resulting from the 3° miscut angle of the NGO substrate [cf. the profile in Fig. 1(c)]. This evidences a perfect crystal growth. The preferential orientation of the steps is compatible with inplane epitaxial growth, while out-of-plane epitaxy is also evidenced by XRD (see Supplemental Material [26]). High-resolution transmission electron microscopy measurements (see Supplemental Material [26]) indicate homogeneous growth of $CaRuO_3$ without any indication of secondary phases or grain boundaries.

The excellent quality of our thin films is corroborated by the observation of Shubnikov–de Haas (SdH) oscillations

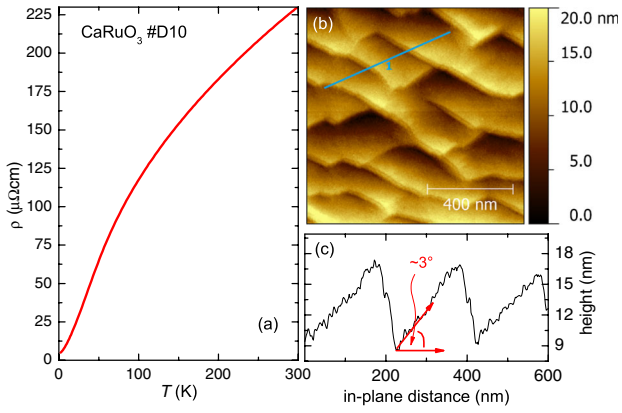

FIG. 1 (color online). (a) Temperature dependence of the electrical resistivity of a 77-nm thin film of $CaRuO_3$. (b) Topography of a (1×1)-μm^2 square as determined by room-temperature STM. (c) Corresponding height profile along the direction indicated by the blue line from right to left in (b).

in the low-temperature magnetoresistance of $CaRuO_3$. Measurements of two different samples, up to 18 T in a superconducting solenoid and between 25 and 35 T in a high-field electromagnet [Fig. 2(a), see also Supplemental Material [26]], consistently reveal quantum oscillations with a frequency of 470 T, corresponding to a Fermi surface area of 4.5×10^{14} $1/cm^2$ and $k_F = 1.2 \times 10^9$ m^{-1}. The temperature dependence of the SdH amplitude follows the expected Lifshitz-Kosevich behavior with an effective mass $m^\star = 4.4\, m_e$ [Fig. 2(c)]. Simultaneous observation of a quadratic resistivity below 1.5 K (discussed below) proves that the material is a Fermi liquid, which overrules pictures explaining the unusual properties in terms of the NFL ground state.

We computed the fermiology of $CaRuO_3$ with the density functional theory within local density approximation (LDA) (see Supplemental Material [26]). LDA reveals many Fermi surface sheets that cover the frequency range between 0.1 and 1 kT quite densely, with some additional long orbits extending (depending on the field direction) up to 10 kT. While the observed data could only be fitted assuming several separate frequencies, the limited number of oscillations does not allow their precise determination. In

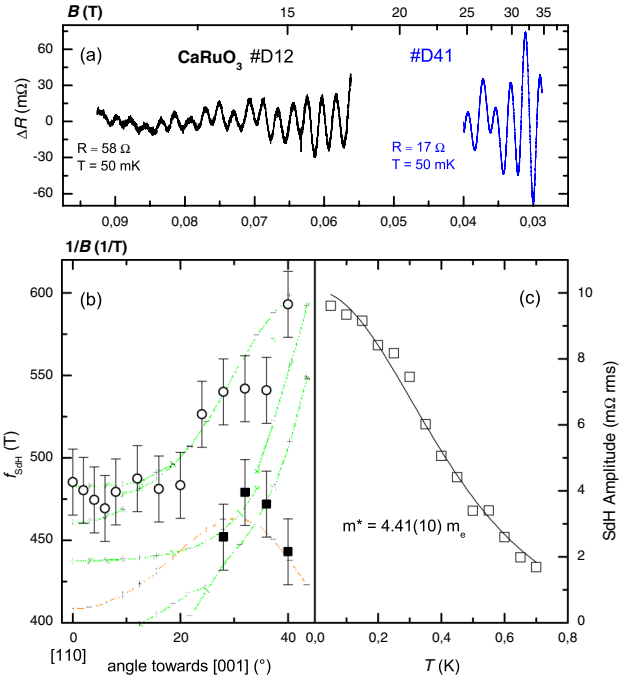

FIG. 2 (color online). (a) SdH oscillations as obtained by subtraction of a second-order polynominal from the isothermal magnetoresistance of $CaRuO_3$ at 50 mK for two different thin films at two different field ranges for $B \| (110)$. (b) Angular dependence of the oscillation frequencies (closed squares indicate additional frequency in tilted field) as determined between 25 and 33 T compared to the local-density approximation (LDA) prediction (lines). (c) Temperature dependence of the SdH amplitude for sample D12. Solid line indicates fit to the Lifshitz-Kosevich formula yielding an effective mass of $4.4\, m_e$.

addition, rotating the field out of the direction perpendicular to the thin-film plane results in a decrease of the SdH signal, and beyond about 40°, its disappearance. Comparison with LDA band structure suggests that the observed two frequency branches belong to extremal orbits of Fermi surface sheets δ_2 and β_3 (see Supplemental Material [26]). The LDA masses of both orbits are about $1.0\,m_e$. The observed mass enhancements due to correlations, ~4.4 and ~4.2 for the former and latter orbit, respectively, are thus a bit smaller than the average enhancement, ~7.0 at zero field, estimated from the experimental specific heat coefficient of 73 mJ/mol K^2 [28]. Interestingly, assuming a Kadowaki-Woods relation $m^\star \propto \gamma \propto A^{1/2}$, the reduction of A by a factor of 2 between 0 and 16 T (see below) accounts for most of the difference between the "specific heat mass" and the effective mass observed by SdH oscillations. The field dependence of the oscillation amplitude (not shown) yields an electronic mean free path of 40 nm, characteristic for a clean metal, and a quasiparticle scattering time of $\tau_{qp} \sim 1.3$ ps. Using the transport lifetime $\tau_{transp} = Z\tau_{qp}/2$ (taking for Z the inverse mass enhancement), the conductivity evaluated from the band theory is ~4 $\mu\Omega$ cm, consistent with the residual resistivity of our samples.

In Fig. 3(b), we show the temperature-dependent part of the electrical resistivity, $\Delta\rho(T) = \rho(T,B) - \rho_0(B)$, down to 50 mK. At low T, the data perfectly follow $\Delta\rho(T) = A(B)T^2$, see also Supplemental Material [26]. However, this FL behavior is limited to temperatures below a tiny T_{FL}. At zero magnetic field, $T_{FL} = 1.5$ K [cf. Fig. 3(d)] is not only small compared to other oxides (e.g., vanadates and molybdates with $T_{FL} > 100$ K) but is also substantially smaller than $T_{FL} = 7$ K found in $Sr_3Ru_2O_7$ [8]. Taking into account that the strength of correlations as suggested by the specific heat enhancement in $Sr_3Ru_2O_7$ is actually larger (about 10, at zero field), the FL behavior in $CaRuO_3$ is surprisingly fragile.

The low coherence scale T_{FL} increases strongly in the magnetic field, while the coefficient A is reduced by a factor of 2 between 0 and 16 T [Fig. 3(c)]. This behavior is opposite to what is found in $Sr_3Ru_2O_7$, where T_{FL} decreases in the magnetic field in response to the field-enhanced spin fluctuations driven by the proximity to a metamagnetic critical point. In $CaRuO_3$, the increase of T_{FL} in a magnetic field suggests, rather, a suppression of the magnetic fluctuations and the associated spin entropy. This may hint at the proximity to a zero-field QCP.

We now address the data beyond the FL regime. Above T_{FL}, the resistivity exponent decreases smoothly from 2 to lower values, cf. Fig. 3(e). In agreement with previous reports [12,14], we can satisfactorily describe the behavior by a $T^{3/2}$ dependence, as evidenced in Fig. 3(a) where ρ plotted vs $T^{3/2}$ appears as a straight line in a broad range up to ~25 K (see also Supplemental Material [26]). The NFL contribution to the electrical resistivity in this temperature regime is large compared to the residual resistivity of our

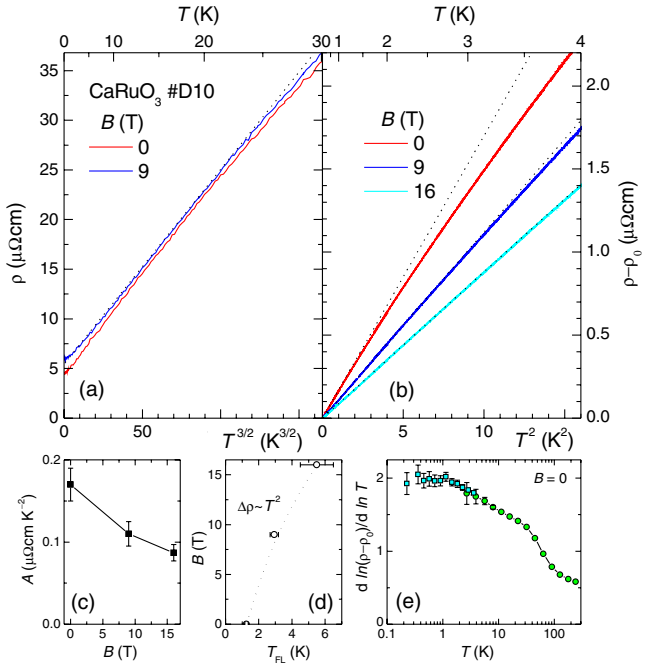

FIG. 3 (color online). (a) Electrical resistivity of $CaRuO_3$ vs $T^{3/2}$ at zero field and a field of 9 T applied transverse to the film plane. Dotted straight line indicates $T^{3/2}$ dependence. (b) Low-temperature (between 50 mK and 4 K) electrical resistivity as $\rho - \rho_0(B)$ vs T^2 for various fields. Dotted black lines indicate Fermi liquid behavior. (c) Coefficient A from $\rho - \rho_0 = AT^2$ behavior vs magnetic field. (d) Phase diagram indicating the existence range of Fermi liquid T^2 behavior in the electrical resistivity, given by the maximal temperature below which the data and straight lines in Fig. 3(b) overlap within noise level. (e) Temperature dependence of the electrical resistivity exponent $d\ln(\rho - \rho_0)/d\ln T$ on a logarithmic temperature scale.

high-quality thin film [at 25 K, $\Delta\rho \sim 7\rho_0$, cf. Fig. 3(a)]. Such behavior is characteristic for clean NFL metals [3,29–34]. Importantly, it supports the idea that the NFL behavior is intrinsic to $CaRuO_3$ and is not dominated by disorder, e.g., by magnetic clusters in a paramagnetic environment [35]. Interestingly, the exponent of 1.5 is similar to that found in the NFL state of MnSi [33], but it is different from the expectation from the itinerant Hertz-Millis-Moriya theory for 3D ferromagnetic quantum criticality [4]. At still higher temperatures, our data tends to a $T^{1/2}$ dependence, consistent with earlier reports [6].

We now turn to the optical properties. We have evaluated the complex optical conductivity $\hat{\sigma}(\omega) = \sigma_1(\omega) + i\sigma_2(\omega)$ from transmission and phase shift measurements at frequencies 0.2–1.4 THz and temperatures 2–300 K [36] (see also Supplemental Material [26]). Comparable measurements on single crystals are impossible due to reflectivity very close to unity.

The improved sample quality has striking consequences on the THz response. In Fig. 4(a) we show $\sigma_{1,2}$ at $T = 15$ K. At low frequencies, $\sigma_{1,2}$ are fit well by a simple

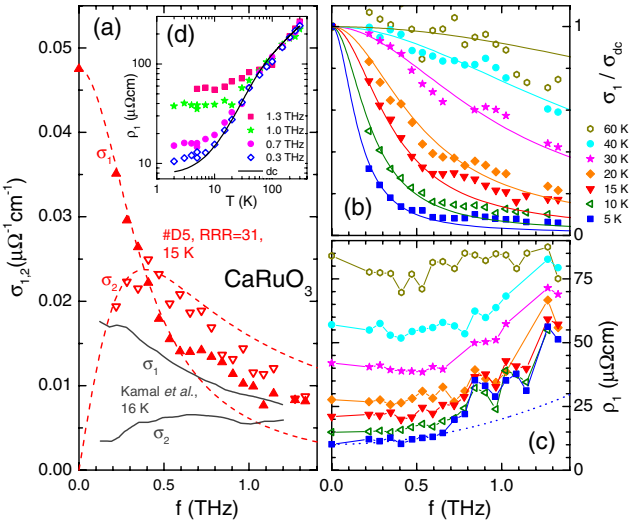

FIG. 4 (color online). THz optical response of a 40-nm-thick $CaRuO_3$ film grown on (110) $NdGaO_3$. (a) Real and imaginary parts of optical conductivity at 15 K (symbols). Dashed lines are a combined Drude fit to σ_1 and σ_2. For comparison, data by Kamal *et al.* are plotted as full lines [7]. (b) Frequency and temperature dependence of σ_1/σ_{dc}, compared to FL model [37]. (c) Frequency and (d) temperature dependence of real part ρ_1 of resistivity [proportional to optical scattering rate $\Gamma(\omega)$]. Dashed line in (c) is a FL prediction for 5 K based on dc data below T_{FL}.

Drude response $\hat{\sigma} = \sigma_{dc}/(1 - i\omega\tau_D)$ with Drude relaxation time τ_D. The crossing of the σ_1 and σ_2 spectra, at $(2\pi\tau_D)^{-1} = 0.4$ THz, signals the transition from the low-frequency dissipative (transport) regime to the inductive (relaxation) regime. For our lowest temperatures, we obtain $\tau_D = 1$ ps, in agreement with the SdH and the dc resistivity values discussed above. At frequencies above 0.6 THz, σ_1 clearly deviates from the Drude prediction. On the high-frequency side, σ_1 and σ_2 meet again, indicating that the scattering has increased strongly. Comparison with data from Ref. [7], also shown in Fig. 4(a), where such dynamic effects can be resolved only with great difficulty, highlights the role of sample quality for these studies.

In Fig. 4(b) we show the frequency dependence of σ_1/σ_{dc} for a set of low temperatures. Upon cooling, the electron-electron contribution to the low-frequency scattering is diminished and the low-frequency Drude roll-off becomes increasingly sharp. At the lowest temperatures measured, the narrowing saturates as the scattering due to electron-electron interactions becomes comparable to the impurity contribution. In the NFL temperature range (2–25 K), the THz data at frequencies below 0.6 THz can be modeled well by a simple Drude response with an ansatz $1/\tau_D = aT^{3/2} + 1/\tau_0$, with $\tau_0 = 1.3$ ps, whereas at higher frequencies all spectra show pronounced deviations from Drude behavior (see Supplemental Material [26]).

Such deviations were recently discussed by Berthod *et al.* who have, assuming FL self-energy, derived a universal dependence of the optical conductivity in terms of a two-parameter scaling function [37]. In particular, a non-Drude foot in σ_1 and two crossings between σ_1 and σ_2 were discussed there, in qualitative resemblance to our data. In the low-frequency regime, Drude behavior is recovered. As shown in Fig. 4(b), our overall data can be fit remarkably well with this theory, yielding a coherence scale $T_0 = 150$ K and an impurity scattering $Z\Gamma = 0.3$ meV. However, the agreement is only in the Drude part. Substantial deviations from Drude dynamics, predicted by that theory, occur only at frequencies too large to directly account for the unusual behavior we find here [26].

To describe these deviations, an extended Drude analysis $\hat{\sigma} = D(\omega)/[\Gamma(\omega) - i\omega]$ can be used, where a frequency-dependent scattering rate $\Gamma(\omega)$ replaces the constant $1/\tau_D$ [38]. In Figs. 4(c) and (d) we evaluate $\Gamma(\omega)$ via $\rho_1(\omega) = \mathrm{Re}[1/\hat{\sigma}(\omega)] \propto \Gamma(\omega)$. For 5 K and frequencies below 0.6 THz, ρ_1 is almost constant, but for higher frequencies a pronounced increase of ρ_1 is found. This abrupt increase is incompatible with the quadratic FL prediction, calculated from the dc transport A prefactor below T_{FL}, as indicated by the dotted line in Fig. 4(c), while the data below 0.6 THz is in perfect agreement with the FL increase. A weaker power-law exponent 3/2, which describes well the temperature dependence in this regime, is even more incompatible with the data above 0.6 THz. For higher temperatures, the strong frequency dependence of $\Gamma(\omega)$ is lost and ρ_1 basically coincides with the dc resistivity throughout our frequency range, as evident from Fig. 4(d).

To conclude, we have grown high-quality thin films of $CaRuO_3$ that display quantum oscillations for the first time for this ruthenate. Electrical resistivity indicates an extended NFL regime that crosses over to FL behavior only below 1.5 K. The optical data reveal a Drude response that at frequencies below 0.6 THz can be modeled with FL concepts. Pronounced deviations from FL behavior are found above 0.6 THz, where an abrupt increase of the scattering might signal the coupling to soft spin fluctuations, a scenario that could be tested by looking at the optical properties as a function of the magnetic field.

We thank H. Schuhmann and M. Seibt for their assistance using the transmission electron microscope and M. Dressel for supporting the THz study. The work was supported by the DFG through SFB 602 and FOR 960. J. M. acknowledges the Slovenian research agency program P1-0044.

*Present address: Institut für Festkörperphysik, Technische Universität Wien, 1040 Wien, Austria.
†Present address: Experimentalphysik VI, Center for Electronic Correlations and Magnetism, Institute for Physics, Augsburg University, D-86135 Augsburg, Germany.

[1] R. A. Cooper, Y. Wang, B. Vignolle, O. J. Lipscombe, S. M. Hayden, Y. Tanabe, T. Adachi, Y. Koike, M. Nohara, H. Takagi, C. Proust, and N. E. Hussey, Science **323**, 603 (2009).

[2] S. Kasahara, T. Shibauchi, K. Hashimoto, K. Ikada, S. Tonegawa, R. Okazaki, H. Shishido, H. Ikeda, H. Takeya, K. Hirata, T. Terashima, and Y. Matsuda, Phys. Rev. B **81**, 184519 (2010).

[3] N. D. Mathur, F. M. Grosche, S. R. Julian, I. R. Walker, D. M. Freye, R. K. W. Haselwimmer, and G. G. Lonzarich, Nature (London) **394**, 39 (1998).

[4] H. v. Löhneysen, A. Rosch, M. Vojta, and P. Wölfle, Rev. Mod. Phys. **79**, 1015 (2007).

[5] P. Kostic, Y. Okada, N. C. Collins, Z. Schlesinger, J. W. Reiner, L. Klein, A. Kapitulnik, T. H. Geballe, and M. R. Beasley, Phys. Rev. Lett. **81**, 2498 (1998).

[6] Y. S. Lee, J. Yu, J. S. Lee, T. W. Noh, T. H. Gimm, H. Y. Choi, and C. B. Eom, Phys. Rev. B **66**, 041104 (2002).

[7] S. Kamal, D. M. Kim, C. B. Eom, and J. S. Dodge, Phys. Rev. B **74**, 165115 (2006).

[8] L. Capogna, A. P. Mackenzie, R. S. Perry, S. A. Grigera, L. M. Galvin, P. Raychaudhuri, A. J. Schofield, C. S. Alexander, G. Cao, S. R. Julian, and Y. Maeno, Phys. Rev. Lett. **88**, 076602 (2002).

[9] G. Cao, O. Korneta, S. Chikara, L. E. DeLong, and P. Schlottmann, Solid State Commun. **148**, 305 (2008).

[10] G. Cao, S. McCall, M. Shepard, J. E. Crow, and R. P. Guertin, Phys. Rev. B **56**, 321 (1997).

[11] J. M. Longo, P. M. Raccah, and J. B. Goodenough, J. Appl. Phys. **39**, 1327 (1968).

[12] P. Khalifah, I. Ohkubo, H. M. Christen, and D. G. Mandrus, Phys. Rev. B **70**, 134426 (2004).

[13] K. Yoshimura, T. Imai, T. Kiyama, K. R. Thurber, A. W. Hunt, and K. Kosuge, Phys. Rev. Lett. **83**, 4397 (1999).

[14] M. Schneider, V. Mosneaga, and P. Gegenwart, Phys. Status Solidi B **247**, 577 (2010).

[15] I. I. Mazin and D. J. Singh, Phys. Rev. B **56**, 2556 (1997).

[16] S. Middey, P. Mahadevan, and D. D. Sarma, Phys. Rev. B **83**, 014416 (2011).

[17] A. Georges, L. de'Medici, and J. Mravlje, Annu. Rev. Condens. Matter Phys. **4**, 137 (2013).

[18] Ph. Werner, E. Gull, M. Troyer, and A. J. Millis, Phys. Rev. Lett. **101**, 166405 (2008).

[19] Z. P. Yin, K. Haule, and G. Kotliar, Phys. Rev. B **86**, 195141 (2012).

[20] N. Kikugawa, L. Balicas, and A. P. Mackenzie, J. Phys. Soc. Jpn. **78**, 014701 (2009).

[21] A. P. Mackenzie and Y. Maneo, Rev. Mod. Phys. **75**, 657 (2003).

[22] A. P. Mackenzie, J. A. N. Bruin, R. A. Borzi, A. W. Rost, and S. A. Grigera, Physica (Amsterdam) **481**, 207 (2012).

[23] C. B. Eom, R. J. Cava, R. M. Fleming, J. M. Phillips, R. B. van Dover, J. H. Marshall, J. W. P. Hsu, J. J. Krajwski, and W. F. Peck, Jr., Science **258**, 1766 (1992).

[24] L. Klein, L. Antognazza, T. H. Geballe, M. R. Beasley, and A. Kapitulnik, Phys. Rev. B **60**, 1448 (1999).

[25] M. Wissinger, D. Fuchs, L. Dieterle, H. Leiste, R. Schneider, D. Gerthsen, and H. v. Löneysen, Phys. Rev. B **83**, 144430 (2011).

[26] See Supplemental Material at http://link.aps.org/supplemental/10.1103/PhysRevLett.112.206403 for details concerning thin film synthesis, structural properties, FL and NFL behavior in electrical resistivity, Shubnikov–de Haas and THz optical measurements, and band structure calculations.

[27] A. P. Mackenzie, J. W. Reiner, A. W. Tyler, L. M. Galvin, S. R. Julian, M. R. Beasley, T. H. Geballe, and A. Kapitulnik, Phys. Rev. B **58**, R13318 (1998).

[28] M. Shepard, S. McCall, G. Cao, and J. E. Crow, J. Appl. Phys. **81**, 4978 (1997).

[29] P. Gegenwart, F. Kromer, M. Lang, G. Sparn, C. Geibel, F. Steglich, Phys. Rev. Lett. **82**, 1293 (1999).

[30] J. Custers, P. Gegenwart, H. Wilhelm, K. Neumaier, Y. Tokiwa, O. Trovarelli, C. Geibel, F. Steglich, C. Pepin, and P. Coleman, Nature (London) **424**, 524 (2003).

[31] J. Paglione, M. A. Tanatar, D. G. Hawthorn, E. Boaknin, R. W. Hill, F. Ronning, M. Sutherland, L. Taillefer, C. Petrovic, and P. C. Canfield, Phys. Rev. Lett. **91**, 246405 (2003).

[32] S. Nakatsuji, K. Kuga, Y. Machida, T. Tayama, T. Sakakibara, Y. Karaki, H. Ishimoto, S. Yonezawa, Y. Maeno, E. Pearson, G. G. Lonzarich, L. Balicas, H. Lee, and Z. Fisk, Nat. Phys. **4**, 603 (2008).

[33] C. Pfleiderer, S. R. Julian, and G. G. Lonzarich, Nature (London) **414**, 427 (2001); N. Doiron-Leyraud, I. R. Walker, L. Taillefer, M. J. Steiner, S. R. Julian, and G. G. Lonzarich, Nature (London) **425**, 595 (2003).

[34] J. A. N. Bruin, H. Sakai, R. S. Perry, and A. P. Mackenzie, Science **339**, 804 (2013).

[35] L. Demkó, S. Bordács, T. Vojta, D. Nozadze, F. Hrahsheh, C. Svoboda, B. Dóra, H. Yamada, M. Kawasaki, Y. Tokura, and I. Kézsmárki, Phys. Rev. Lett. **108**, 185701 (2012).

[36] U. S. Pracht, E. Heintze, C. Clauss, D. Hafner, R. Bek, S. Gelhorn, D. Werner, M. Scheffler, M. Dressel, D. Sherman, B. Gorshunov, K. S. Il'in, D. Henrich, and M. Siegel, IEEE Trans. THz Sci. Technol. **3**, 269 (2013).

[37] C. Berthod, J. Mravlje, X. Deng, R. Žitko, D. van der Marel, and A. Georges, Phys. Rev. B **87**, 115109 (2013).

[38] M. Scheffler, K. Schlegel, C. Clauss, D. Hafner, C. Fella, M. Dressel, M. Jourdan, J. Sichelschmidt, C. Krellner, C. Geibel, and F. Steglich, Phys. Status Solidi B **250**, 439 (2013).